Informatics in Medicine Unlocked 23 (2021) 100522

Contents lists available at ScienceDirect

Informatics in Medicine Unlocked

journal homepage: http://www.elsevier.com/locate/imu

RBBP6 interactome: RBBP6 isoform 3/DWNN and Nek6 interaction is critical for cell cycle regulation and may play a role in carcinogenesis

Zukile Mbita [a,**], Rodney Hull [b], Fortunate Mokoena [b], Chin-Hung Lai [c], Zodwa Dlamini [b,*]

[a] Department of Biochemistry, Microbiology and Biochemistry, University of Limpopo, Sovenga, 0727, South Africa
[b] SAMRC/UP Precision Prevention and Novel Drug Targets for HIV-Associated Cancers (PPNDTHAC) Extramural Unit, Pan African Cancer Research Institute (PACRI), University of Pretoria, 0028, Hatfield, South Africa
[c] Department of Medical Applied Chemistry, Chung Shan Medical University, Taichung, 40241, Taiwan

ARTICLE INFO

Keywords:
RBBP6
DWNN
NEK6
Homology modelling
Protein docking
Cell cycle regulation
Cancer

ABSTRACT

RBBP6 is a multidomain protein, with four splice variants translated into four functional isoforms. RBBP6 isoform 1 has been reported to interact with TP53 and pRb as well as with proteins that regulate transcriptional response to tumorigenesis such as HDM2, ZBTB38, YBX1 and NEK6. Experimental validation of isoforms 2 and 4 is yet to be conducted. The third isoform, consisting of only the DWNN domain and a short unordered c terminus, has been shown to be down-regulated in several human cancers and demonstrated as a regulator of G2/M cell cycle arrest. A number of studies have supported the role of DWNN in cell cycle regulation, however, its mechanism in these processes remains obscure. Posttranslational modification of DWNN could be critical for its function and this study was formulated to understand how the DWNN regulates the cell cycle. Our study identified 12 cell cycle-related proteins interacting with DWNN using various bioinformatics tools. We also identified 10 ubiquitin ligases that interact with DWNN. The most relevant interacting partner, the cell cycle regulator Nek6, has been reported to interact with DWNN during the cell cycle. It was therefore critical to interrogate the interaction between Nek6 and DWNN by homology modelling and docking. The DWNN mutants had a reduced affinity for NEK6 with at least one of the mutants having changes that affect at least one phosphorylation site. It is likely that NEK6 promotes cell proliferation by phosphorylating DWNN. This work suggests that DWNN co-regulates RNA splicing, ubiquitination, and cell cycle control. DWNN may therefore, be targeted for novel anticancer therapies through cell cycle regulation.

1. Introduction

The retinoblastoma binding protein 6 (RBBP6) gene is conserved across a wide range of eukaryotic organisms [1]. Its protein isoforms have been implicated in various biological processes that include cell cycle regulation [2] and mRNA processing [3,4]. In order to facilitate these cellular functions, RBBP6 proteins contain a number of functional domains, which include the N-terminal Domain With No Name (DWNN), zinc knuckle and E3 ligase activity RING finger domain. Through the RING finger domain, RBBP6 has been shown to promote MDM2-mediated ubiquitination and proteasomal degradation of p53 [5] and the pro-proliferation transcription factor, box binding Protein 1 (YB-1) [6]. Additionally, due to its E3 ligase activity, RBBP6 ubiquitinates a transcription repressor, zinc finger and BTB domain containing 38 (ZBTB38), which controls the levels of replication factor mini-chromosome maintenance 10 (MCM10). Consequently, the knockdown of RBBP6 led to reduced replication fork movement [7]. In addition to classical domain configuration, the mammalian RBBP6 comprises of the retinoblastoma (Rb)-binding, p53-binding domains, proline-rich and serine rich regions. In fact, RBBP6 was first identified in mouse as Rb- [8,9] and p53-binding protein [10] from which it derived names such as p53-associated cellular protein testes derived (PACT) and proliferation potential-related protein (P2P-R or PP-RP) [11].

RBBP6 has been demonstrated to be essential for cell viability, as its absence leads to early embryonic lethality in mice [5], flies [12] and worms [13]. Knock-down of truncated derivative of RBBP6 in mice was shown to significantly decrease the p53-Hdm2 interaction, reducing p53 poly-ubiquitination and degradation, and thereby enhancing p53

* Corresponding author.
** Corresponding author.
E-mail addresses: Zukile.Mbita@ul.ac.za (Z. Mbita), Zodwa.Dlamini@up.ac.za (Z. Dlamini).

https://doi.org/10.1016/j.imu.2021.100522
Received 27 August 2020; Received in revised form 13 January 2021; Accepted 13 January 2021
Available online 20 January 2021

accumulation [5]. The accumulation of p53 leads to both apoptosis and cell growth retardation. Overexpression of RBBP6 in mice leads to apoptosis [14,15] and equally, silencing of RBBP6 variant 1 by RNA interference technology in mouse 3T3 cells led to resistance towards camptothecin-induced apoptosis [16]. In humans, the single copy of RBBP6 gene is found on chromosome 16p12.2 encoding four protein isoforms due to alternative splicing and poly-adenylation (Fig. 1). Human RBBP6 is a promising target for cancer immunotherapy, its upregulation was strongly correlated with cervical [17], gastric [18], colon [19] and lung [20] cancer progression. Indeed, enhanced levels of RBBP6 correlates with poor clinical progression and has been linked to low survival rates in esophageal cancers [21]. Furthermore, cytotoxic T-cells specific to RBBP6 derived peptides were able to lyse cultured esophageal cancer cells and regress esophageal tumors in mouse xenograft models [1].

At present, not much is known about the role of DWNN, which is strictly found at the N-terminus of RBBP6 proteins and, through the use of alternative polyadenylation sites is spliced into an independent module, referred to as RBBP6 isoform 3 (Fig. 1) [22–24]. Although RBBP6 isoform 3 is comprised of the DWNN domain (1–76) and an unstructured C-terminal region, only the DWNN domain which adopts a ubiquitin-like fold has been resolved by nuclear magnetic resolution (NMR) [1]. The DWNN domain has been shown to mediate an interaction to cleavage stimulation factor (CstF-64), in which the other RBBP6 isoforms and RBBP6 isoform 3 compete for binding [3]. Overexpression of isoform 3 inhibits the cleavage of newly synthesized mRNA, raising intriguing possibilities of modulation of 3' processing by fine tuning the levels of the two RBBP6 isoforms. Furthermore, RBBP6 isoform 3 appears to be involved in both cell cycle regulation and camptothecin (CPT)-induced apoptosis. Also, higher expression levels of isoform 3 were seen in colorectal, breast, cervical, ovarian, and prostate cancer when compared to normal samples. This expression was also localized to regions with increased levels of apoptosis [24]. The expression of RBBP6 isoform 3 is known to be high in certain cancers such as esophageal, colon and uterine [24]. While the expression of isoform 1 can be described as low to medium in most cancers [25] (proteinatlas.org/ENSG00000122257-RBBP6/pathology). Differences in the expression of these isoforms has been determined through the use of antibodies developed against DWNN determined that isoform 1 is expressed at much lower levels than isoform 3. This is possible because isoform 3 appearing as a 10 kDa band and isoform 1 as a 200 kDa band. In addition to this, detection intensity using antibodies specific to DWNN has been compared to the intensity in the same samples using antibodies specific for the other regions of RBBP6 not found in isoform 3 but present in isoform 1,2 and 4 [26].

Importantly isoform 3 lacks the nuclear localization signal (Fig. 1). However, while isoform 3 is found predominantly in the cytoplasmic extracts from cells not exposed to stress. The nuclear expression of isoform 3 increases following exposure of the cells to stress conditions in the form of heat or DNA damage [26]. Following stress RBBP6 isoform 3 localises to nuclear speckles which also contain the splicing factor SC35 (Spector [27], and are implicated in DNA damage repair and mRNA processing ([28].

Taken together, the difference in the expression of the two isoforms of RBBP6, isoform 1 and 3 during cancer progression, combined with their competition for binding Cst64 during mRNA processing suggest that the two isoforms do not play complimentary roles. We suspect that the low expression of RBBP6 isoform 3 in cancer cells may facilitate the evasion of cell cycle control and apoptosis. Indeed, a number of studies have suggested that RBBP6 plays a role in the regulation of cell cycle, although the mechanism remains unclear. The focus of this study is to identify proteins that potentially interact with RBBP6 isoform 3 and investigate its interaction with Nek6. Nek6 is one of the 11 members of the Nima (never in mitosis, gene A)-related kinases (Neks) family serine/threonine kinases. These share 40–45% amino acid sequence identity to *Aspergillus nidulans* mitotic regulator, NIMA, within their catalytic domains. Neks play important roles in cell cycle regulation and have recently been described as playing an important role in pathologies such as cancer. Human Nek6, 7 and 9 are involved in the control of mitotic spindle formation [29].

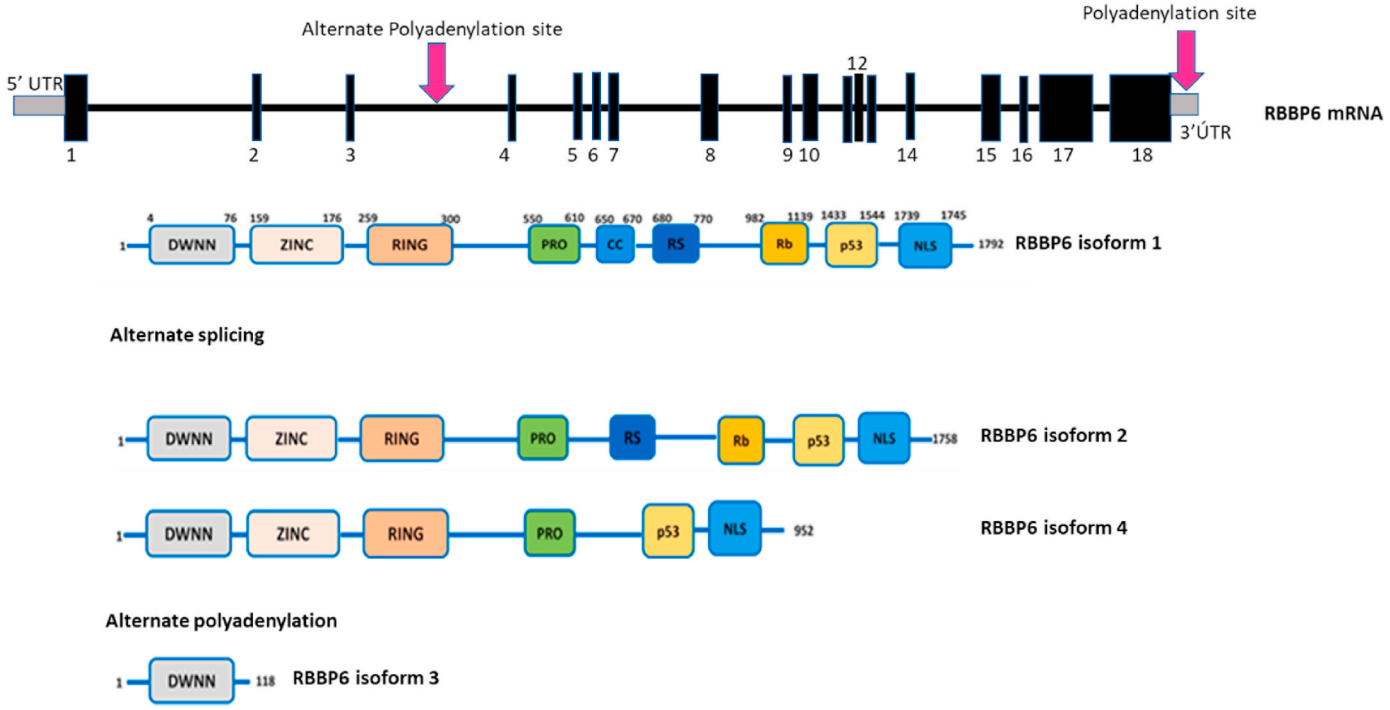

Fig. 1. Schematic diagram of RBBP6 isoforms. This figure depicts the domain structure of all four RBBP6 isoforms. Isoforms 2 and 4 arise from alternate splicing. Isoform 3 arises from the use of an alternate polyadenylation site after exon 3. Adapted from Refs. [22–24].

2. Materials and methods

The computational framework used for studying the interaction of RBBP6 isoform 3 (NP_116,015) with other proteins is given in Fig. 2. Briefly, the RBBP6 isoform 3 interaction network construction and annotation, homology modelling and protein-protein docking were done using various bioinformatics tools, namely, KEGG, PFAM, CDD, NetPhos, KinasePhos, Modeler, ClusPro and Haddock. The proteins interacting with RBBP6 isoform 3 were mapped on KEGG and classified using PFAM. They were then aligned using CDD-BLAST. Kinase predictions was conducted with the use of KinasePhos and NetPhosK. The Nek models were built using Modeler and lastly, protein-protein docking was conducted using ClusPro and Haddock.

2.1. Protein-protein interaction network

To obtain a proper perspective of the RBBP6 isoform 3 protein-protein interaction network, a literature based search for experimentally detected partner proteins was constructed by combining hits obtained from the following databases: BioGrid [30,31], DIP [32], HPRD [33], InnateDB [34] and IntAct [35]. These open source PPI databases are populated with manually curated protein-protein interaction data for all model organisms. In addition, the StringDB repository, which contains predicted protein interactions obtained from direct (physical) and indirect (functional) associations [36,37], was also searched for proteins interacting with RBBP6. Searching these databases using RBBP6 isoform 3 (Accession number: NP_116015.2) led to no interactions. Therefore, the full length RBBP6 isoform 1 (Accession number: NP_008841.2) was used as a query. The overlapping proteins that were returned from these multiple databases were used to construct a network of interacting proteins. This network of proteins was then refined by removing those proteins that were predicted to interact with RBBP6 isoform 1 through its p53, RB1, RING finger or Zinc finger domains. In addition to this the proteins that were determined to experimentally interact with RBBP6 isoform 1 were also removed. The remaining protein sequences and data were obtained from Uniprot [38]. These proteins were then functionally enriched by using them as queries in the KEGG pathway database which mapped each protein to canonical pathways and families [39]. Proteins involved in the cell cycle and ubiquitination were selected for further analysis. This resulted in a group of proteins involved in the cell cycle and ubiquitination that would presumably only interact with the DWNN domain, and therefore these proteins and not the excluded proteins could interact with RBBP6 isoform 3. PFAM was used to search and classify the queries into protein families using the large and comprehensive collection of proteins families which are each represented by multiple sequence alignment and hidden Markov models (HMMs) profiles [40]. The CDD-BLAST resource contains well-annotated multiple sequence alignment models for ancient domains and full length proteins. It relies of RPS-BLAST, a modified version PSI-BLAST to quickly scan a set of pre-determined position-specific score matrices (PSSMs) with a protein query [41,42].

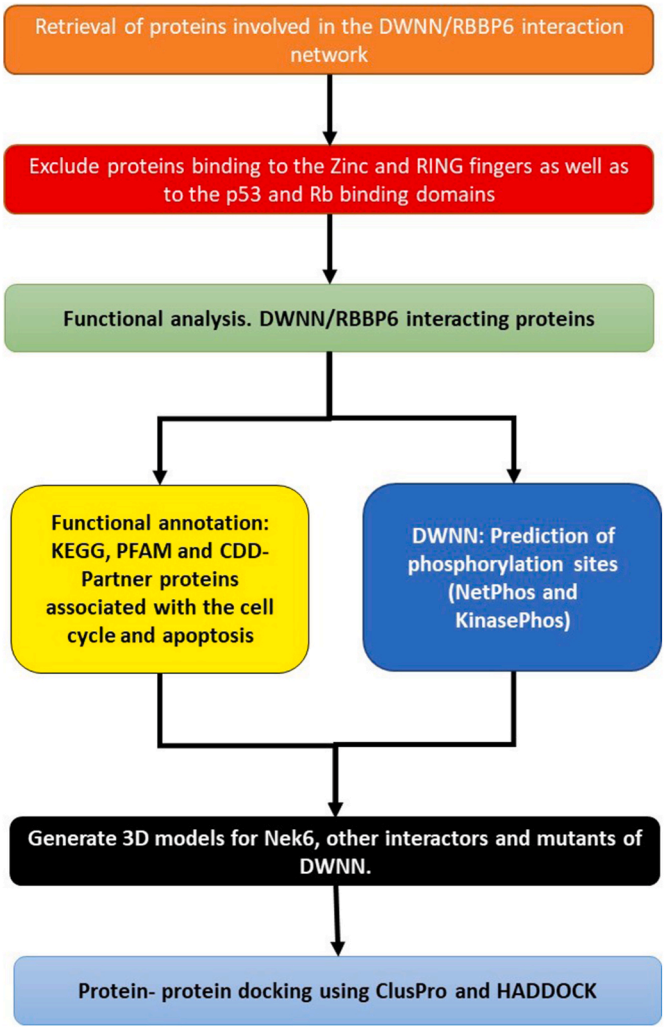

Fig. 2. Computational framework used to identify the partner proteins of RBBP6 and characterize its interaction with Nek6.

2.2. Mutagenesis and homology modelling

The phosphorylation sites of DWNN were predicted using Kinasephos 2.0, a kinase-specific phosphorylation site prediction tool, which adapts the sequence-based amino acid coupling-pattern analysis and solvent accessibility [43] and NetPhosK 1.0 server that generates NN predictions of kinases specific eukaryotic protein phosphorylation sites [44]. Homology modelling was done for Nek6 (Uniprot accession: Q9HC98) as well as the other proteins with no crystal or NMR structure that were identified as closely interacting with RBBP6 isoform 3. Namely, MZT2 (Uniprot accession Q6NZ67), GINS2 (Uniprot accession Q9brt9), RNF115 (Uniprot accession Q9Y4L5), MAX (Uniprot accession P61244), UBE2L2 (Uniprot accession Q7Z7E8), RLIM (Uniprot accession Q9NVW2), PRKAA (Uniprot accession Q13131), CUL5 (Uniprot accession Q93034), TRIP12 (Uniprot accession Q14669), UBE2L3 (Uniprot accession P68036) and UBE2Q2 (Uniprot accession Q8WVN8).

Homology modelling was also performed on other cell cycle regulation proteins, identified to interact with RBBP6 isoform 3. These included PLK1 (Uniprot accession 014,777), PRKAA1 (Uniprot accession Q12121), SMAD3 (Uniprot accession P48022), MAX (Uniprot accession P61242) and MZT2 *Uniprot accession Q6ZN7). The template utilized for modelling Nek6 (Nek7 PDB ID: 2WQM) was identified using HHPred webserver [45]. The PROfile Multiple Alignment with predicted local structures and 3D constraints (PROMALS3D) alignment tool [46] was then used to generate an accurate target to template alignment. The models were built using MODELER 9v18 with slow refinement [47]. Loop refinement was also carried out to predict the most plausible 3D model of Nek6 with the least stereo-chemical violations [48]. Hundreds of models were generated for each protein and ranked on the basis of energy score. The best three models were selected by DOPE Z score calculations. Final evaluations were performed using RAMPAGE [49,50], Verify3D [51] and ProSA [52]. The Nek6 model had a Z Score of 0.76 and a QMEAN score of −2.66 while the RBBP6 isoform 3 model has a Z score of 0.63 and a QMEAN score of −2.68. These models therefore show a good fit with experimental model structures.

2.3. Protein-protein docking

Protein-protein docking studies were carried out by docking the

RBBP6 isoforms 3 homology model with the 3 D models obtained for NEK6, MZT2, GINS2, RNF115, MAX, UBE2L2, RLIM, PRKAA, CUL5, TRIP12, UBE2L3 and UBE2Q2 using ClusPro V2 [53,54] and HADDOCK [55,56]. Protein data bank files were downloaded for the other proteins that RBBP6 isoform 3 interacts with and did not therefore require 3D modelling. These included TUBG1 (Uniprot accession P23258), NDC80 (Uniprot accession O14777), UBE2G2 (Uniprot accession P60604), CHMP4B (Uniprot Accession Q9H444, UBE2Q1 (Uniprot accession Q7Z7E8), RNF126 (Uniprot accession Q9BV68), PCNA (Uniprot accession Q15004) and HECW2 (Uniprot accession Q9P2P). To remove false positives, we selected the first 20 poses from ClusPro server (comprise of a cluster of 10 poses and 10 poses of favourable hydrophobic interactions) and top 10 poses from HADDOCK for evaluation using with Dock Score server [57]. The structural analysis of protein-protein interface interactions, details of contacts, and the statistics, were carried out on PDB sum webserver [58,59]. Moreover, residues involved in probable hydrophobic interactions, hydrogen bond and electrostatic interactions were determined using the Protein Interaction Calculator (PIC) webserver [60]. ClusPro models where interacting residues were identified were illustrated showing amino acid side chains involved in the interaction using Swiss-PDB viewer.

2.4. Analysis of DWNN mutants and phosphorylation

Additionally, homology modelling was performed for the two RBBP6 isoform 3 mutants, S25A and T49A. These mutants which were modelled from the wildtype NMR structure of DWNN (PDB ID: 2C7H). The SWISS model program was used to model the change to the 3D structure of DWNN caused by the amino acid changes in the two DWNN mutants, S25A and T49A. The prediction of residues within RBBP6 isoform 3 that could possibly be phosphorylated was carried out by Netphos bioinformatics program [61].

3. Results

3.1. RBBP6 interaction network and enrichment through pathway analysis

Based on the relative lack of knowledge regarding RBBP6 interactions, an effort to construct its protein network map was undertaken by using 6 databases. This resulted in the identification of a total of 133 unique partner proteins across all databases. No hit was obtained from DIP while the interactions derived from three other literature based PPIs InnateDB [62] (28 interactors), IntACT [63] (38 interactors), BioGrid (122 interactors), HPRD [64] (11 interactors) and StringDb (10 interactors). Of all these interactors 133 unique proteins overlapped across all databases (Table 1). This network of 133 human and mice interactors with RBBP6 [5,6,10,65–80] were further refined by isolating proteins that only interact with the DWNN domain. This would allow us to better characterize the role of RBBP6 isoform 3 through its protein interactions, all interactions that occur through partner proteins, which interact with RBBP6, such as p53, RB1, the RING finger as well as experimentally verified interactions, were removed. The remaining protein sequences and data were obtained from Uniprot [38].

Table 1
Stages in the identification of proteins predicted to interact with RBBP6 isoform 3 through the DWNN domain.

Database searches					
Biogrid	Innate db	Intact	STRINGDB	HPRD	DIP
122	**28**	**38**	10	**11**	0
Unique proteins across all databases				133 proteins	
Proteins interacting with the DWNN domain				83 proteins	
Pathways enriched using KEGG analysis					
Cell Cycle proteins			24 proteins		
Ubiquitin ligases			10 proteins		
Apoptosis			2 proteins		
Metabolism			6 proteins		
mRNA processing			24 proteins		
MAPK			7 proteins		
FOXO signalling			10 protein		

The KEGG analysis of RBBP6/DWNN interacting proteins revealed that the 6 significantly enriched pathways were metabolism, mRNA surveillance, ubiquitin mediated proteolysis, cell cycle, MAPK and FOXO signalling pathways. These findings are consistent with experimental studies which have implicated all the isoforms of RBBP6 (through the DWNN domain) in mRNA surveillance, ubiquitin mediated proteolysis and MAPK signalling pathway. It is important to note that as all the isoforms of RBBP6 have the DWNN domain, the interaction between Nek6 and the DWNN domain is not unique to isoform 3. This is true of all the identified interacting proteins. However, the interaction of isoform 3 with these proteins may serve to regulate the interaction of the other isoforms with these proteins by competing for binding sites. Additionally, if these proteins are a target for DWNNYlation, Isoform3 may not only inhibit the binding of the other RBBP6 isoforms to the identified proteins but may also lead to their degradation. . These proteins were analyzed further.

3.2. mRNA processing

Polyadenylation of mRNA precursors is a crucial step in the synthesis of functional eukaryotic mRNAs and is facilitated by a large multisubunit protein complex. RBBP6 isoform 1 and RBBP6 isoform 3 (through the DWNN domain) have been implicated as regulators of 3′mRNA processing with AU-rich UTRs such as c-Fos and c-Jun [1,3]. All RBBP6 isoforms are suspected of associating with core factors of the mRNA processing; CPSF1, CPSF2, CPSF4, CPSF6, CSTF2 and CSTF3 [3]. This interaction is mediated by the ubiquitin-like domain, DWNN which has been shown to out compete RBBP6 for binding to CstF64 (CSTF2) [3]. It has also been suggested that RBBP6 interacts with Pinin [81], which binds to the E-box 1 core sequence of E-cadherin which leads to the promotion of gene transcription. The stringDB identified two Trp-Asp (WD) repeat containing proteins (WDR33 and WDR82) and another component of the cleavage and polyadenylation factor (CPF) complex, RNA polymerase II subunit A C-terminal domain phosphatase SSU72 as interacting partners of all isoforms of RBBP6 through the/DWNN domain. The molecular architecture and dynamics of the 3′ processing complex remains poorly understood, we therefore, suggest that experimental validation of these interactions to RBBP6 isoform 3 may serve as an important step towards this understanding. It is possible that RBBP6 along with Pinin, WDR82, WDR33 and the known CPF complex factors constitute a functional mRNA processing complex.

3.3. Ubiquitin mediated proteolysis and cell cycle regulation

StringDB mapped 11 more unique protein partners of RBBP6 (Fig. 3A). These proteins are all involved in ubiquitination and are E2 or E3 ubiquitin ligases. The proper control of the levels of proteins within a cell is vital to the proper functioning of an organism. The proper regulation of protein degradation is vital for the correct functional of molecular pathways within an organism in living organisms. Indeed, ubiquitination regulates apoptosis, antigen processing, DNA repair, protein quality control, signal transduction and stress response [82,83]. It has been specified that over 600 human genes contain the RING-based E3 ligase domain which transfers ubiquitin from an E2 ubiquitin ligase to a target protein. Indeed, RBBP6 isoforms other than isoform 3 contain a RING finger and has been proposed to play a role as an E3 ligase, and has been found to be involved in protein degradation by binding to one of the four subunits of the ubiquitin protein ligase called SKP1-cullin-F-box (SCFs) of the ubiquitin ligase FBXO7 [67]. It has been suggested that the RING finger domain of RBBP6 mediates an interaction with ubiquitin conjugating enzyme UBE2I which also interacts with

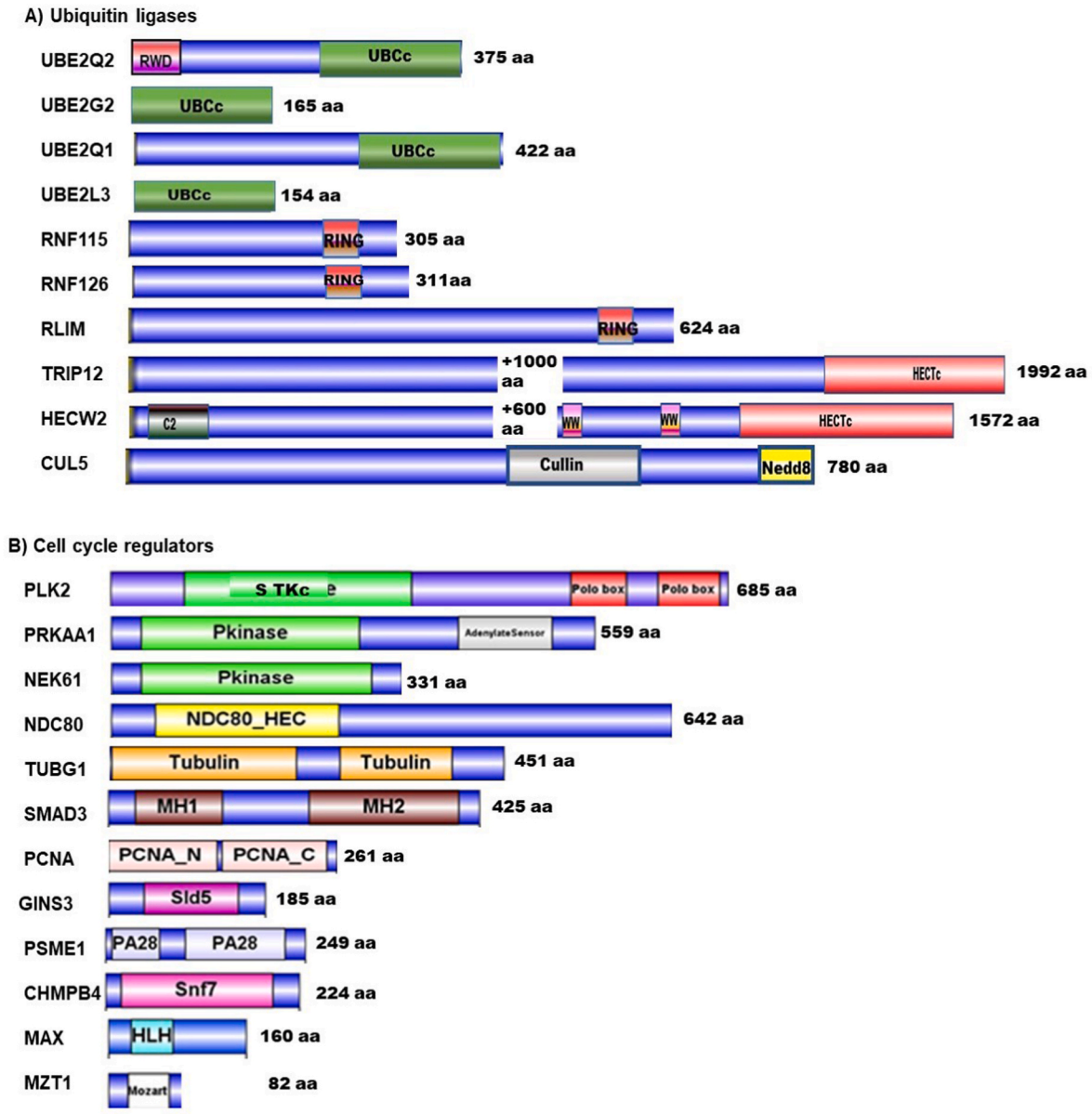

Fig. 3. Cell cycle and ubiquitin ligase related proteins interacting with RBBP6 isoform 3/DWNN. This figure shows the basic domain structure of the **(A)** 10 Ubiquitin ligases and the (B) 11 cell cycle regulators that were predicted to interact with RBBP6-isoform 3.

p53. Although most studies have focused on the role of RBBP6 isoform 1 in ubiquitination, the, DWNN has been shown to be similar to ubiquitin since it is superimposable with ubiquitin. Ubiquitin tags proteins for degradation by the proteasome [1]. The interaction between DWNN and heat shock protein HSPA14 supports the hypothesis that DWNN is involved in chaperone mediated ubiquitination of unfolded proteins [80]. The possibility that DWNN interacts directly with HECW2, PSME1, UFL1 and UFM1 remains to be experimentally validated. RBBP6 isoforms through the DWNN domain, probably co-regulate p53 activity by ubiquitination and possibly the transfer of a DWNN group to the protein, a process that can be easily coined as "DWNNlyation".BBP6 also plays a role in important cellular processes such as cell cycle control, because it has been shown to interact with cell cycle related proteins MAD2L2 [84] and the spindle-regulating protein TPT1 [85]. Protein-protein interaction network predictions found 12 cell cycle-related proteins possibly related to DWNN (Fig. 3B).

3.4. Homology modelling of Nek6

The 3D structural model of human Nek6 was constructed using the 3D structure of human Nek7, which was determined experimentally using crystallography. This structure was obtained from the PDB database (PDB entry 2WQM) and used as a template [86]. Nek7 is able to play the role of a template as it shares approximately 77% sequence identity with Nek6 **(**Fig. 4 **A)** and ~86%, within the catalytic domains. Based on the sequence alignment, a truncated model of Nek6 was constructed (starting at residue 21). Following loop refinement, the primary 3D model of Nek6 resulted from the homology modelling as shown in Fig. 4 B and **C.** Based on the model quality assessment and stereochemistry quality analysis, our model is improved from Merielles et al. (2011) and Srinivasan et al. (2014) [29,87]. The Ramachandran plot of the Nek6 model compares well with that of Nek7 showing 88.1% most favourable regions, 11.6% additionally allowed regions and only 0.3% disallowed region (Ser 206) as compared to the template with these values 90.8%, 8.8%, 0.4% and 0.0%, respectively (Fig. S1). It is important to note that the crystallographic structure of Nek7 has

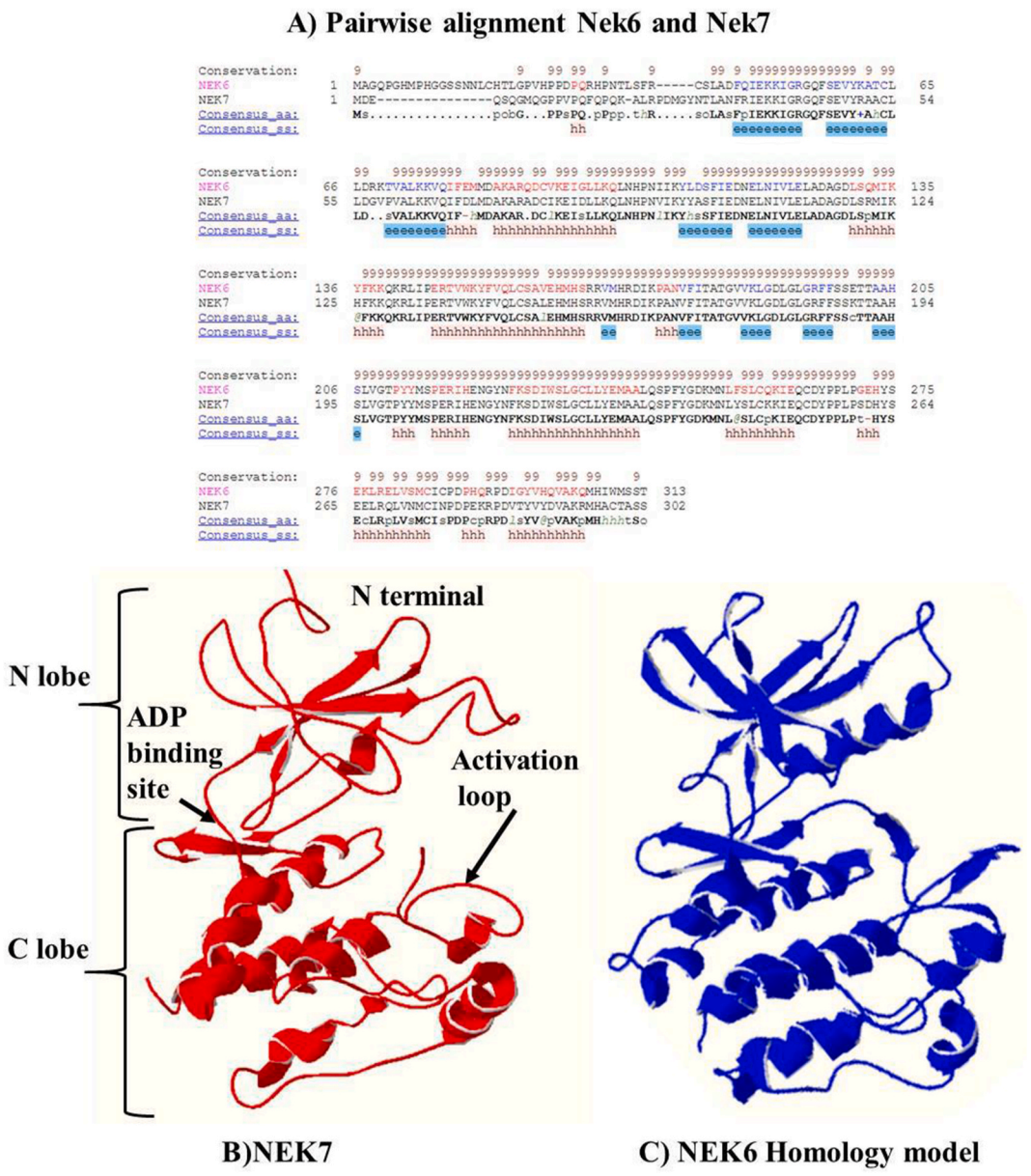

Fig. 4. Homology model of Nek6. (A) The homology modelling used Nek7 as a template (A) the alignment of Nek 7 and Nek6 sequences shows that Nek7 shares approximately 77% sequence identity with Nek6. (B) The 3D structure of Nek 7, showing some important structural feature. (C) The 3D structural model of Nek6 using Nek7 as a template.

relatively long regions where the phases could not be solved by X-ray crystallography [86]. Consequently, the homology modelling may not be so accurate in these regions, although the high identity of the target-template sequences makes the whole model plausible. The results revealed that the majority of the amino acids are in a ψ distribution consistent with a right-handed α-helix and is therefore likely to be a good quality reliable model). Further validation of the predicted model of Nek6 results and its quality assessment were done by comparison to the template using the Z-scores of −7.59 and −7.02 for Nek7 and Nek6, respectively, indicating that the residue energies together with pair energy, combined energy, and surface energy were all negative and had comparable surface energy affinity with template. Altogether, no abnormalities were observed in the validation process, which indicated a good model for the protein.

3.5. Protein-protein docking

Docking analysis between the 3D homology model of Nek6 and the NMR structure of the DWNN domain using ClusPro, resulted in 25 models with energetically and hydrophobically balanced favourable member numbers ranging from 106 to 7. The ClusPro algorithm takes the 1000 models with the lowest energy. It then rotates the ligand (DWNN) within a space of 9 Å and calculates the number of these new variations of the central model are viable positions for docking. These are then presented as a cluster of models and the number of viable models are called cluster or member numbers. Models are then ranked by their member numbers. The most energetically favourable model has 135 members and is only slightly more energetically favourable energy of centre docking model (−679.6), lowest energy configuration (−719.3) than the model with the most members (176 member's energy of centre docking model −544.1, lowest energy configuration −659/01). However, the use of the protein interaction calculator

bioinformatics software [60] showed that these models did not form bonds within the 6 Å (A) cut off. In other words, it only searches for probable bonds that can form between interacting protein sidechains or backbones that can be within 6A of each other. The most energetically favourable model with predicted interactions had 91 members and an energy of centre docking model (−636.6), lowest energy configuration (−681.3). This docking model is shown in Fig. 5.

3.6. Homology modelling of RBBP6 isoform 3 mutants and phosphorylation prediction

Homology modelling of the two mutant forms of RBBP6 isoform 3 were carried out using the NMR structure of DWNN. The results obtained here do not show many structural differences between the mutants and wild type proteins. The wild-type DWNN contains 7 Beta sheets and a single alpha helix. The amino acid substitutions in the mutants S25A and T49A do not cause major changes to the 3D structure of the protein. Residue 25 is located between β1 and β2. However, there is no change to the protein structure in this region. Residue 49 is located at the beginning of the β4 beta sheet. However, the amino acid substitution does not change the structure of the protein. Despite this, the mutants interact very differently with NEK6, as can be seen in Fig. 6A. While S25A interacts in roughly the same region as the wild type protein, T49A binds to a different part of the protein and both mutants bind to the protein with different regions of themselves. These docking models are also more energetically unfavourable than the docking model with the wild type (Table 2). This indicates that these mutant forms of RBBP6 isoform 3 bind to Nek6 less efficiently than the wild type protein. Predictions of the residues of DWNN that may be phosphorylated shows 13 possible phosphorylation sites (Fig. 6B). The Serine at position 25 is one of the regions predicted to be phosphorylated. This residue is substituted with an alanine in the mutant. This alanine is predicted to interact with NEK 6 when the mutant binds to NEK6.

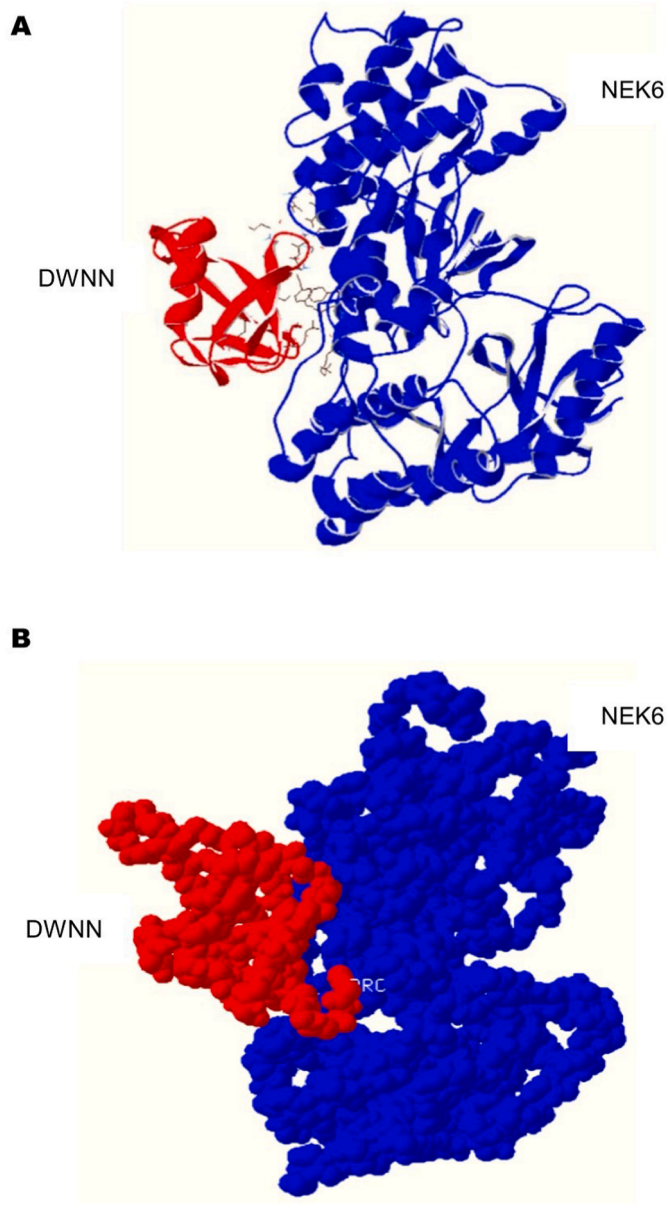

Fig. 5. Docking model for the interaction between Nek6 model and DWNN NMR structure: DWNN interacts with the area of NEK6 that corresponds with the ADP binding site of NEK7. (A) The ribbon structure of the model, showing the sidechains of the DWNN domain and the NEK6 proteins that are involved in the interaction which are shown as stick structures. (B) The space filling model of the interaction.

3.7. Protein docking between RBBP6 isoform 3 and different cell cycle regulators and ubiquitin ligases

ClusPro was used to model RBBP6 isoform 3 interactions with the 12 identified cell cycle regulators that were previously identified as associating with RBBP6 isoform 3 (Fig. 7) and the ubiquitin ligases (Fig. 8) that were identified to interact with RBBP6 isoform 3. Once these models were obtained, they were analyzed using the Protein Interaction Calculator tool (PIC) [60]. Those proteins, which were predicted to form interactors within the 6 Å cut off range are shown in Table 3 and are illustrated in Figs. 7 and 8. Those models that did not show any bonds within the 6 Å cut off were discarded. The cell cycle regulator with the most energetically favourable interactor are all involved with regulating cell division by interacting with microtubules during cell division. These include TUBG1, NDC80, MZT2 and CHMPB4. MAX is a transcription regulator that promotes cell cycle progression. GINS2 is a proteasome component that inhibits progression through the cell cycle [88]. Those E3 ligases that interact with RBBP6 isoform 3 with predicted bond formation are shown in Fig. 8. Three of these proteins are E2 ligases UBE2L2, UBE2Q1 and UBE2L2. The remaining two are both E3 ligases, RNF115 and RLIM.

The remaining cell cycle regulators and ubiquitin ligases were docked with RBBP6 isoform3 using ClusPro. These interactors do not have residues involved in probable hydrophobic interactions, hydrogen bond and electrostatic interactions as determined using the Protein Interaction Calculator (PIC) webserver.

4. Discussion and conclusion

This paper uncovers further interactions of RBBP6 that are vital hallmarks of cancer. Here we show the interaction of protein Nek6 with human RBBP6 isoform 3 and particularly the DWNN domain. Understanding these protein interactions are important to reveal the underlying mechanisms of RBBP6 and its role in RNA splicing, ubiquitination, and cell cycle control.

Similar to most proteins that interact with DNA and play a role as an E3 ubiquitin ligase, RBBP6 contains the RING finger E3 ligase domain which is responsible for ubiquitination. The full length isoform of RBBP6 is generally overexpressed in most cancers and contributes to proliferation. In cancers such as colorectal, breast and cervical, the RING finger E3 ligase domain is often associated with metastasis and poor prognosis [89,90]. Xiao et al. (2019) demonstrated that the RBBP6 activation of the NF-κB pathway induces the epithelial–mesenchymal transition required for metastases [90]. In contrast, RBBP6 isoform 3/DWNN is shown to be downregulated in some cancers and has anti-proliferative activities. Reduced expression of RBBP6 isoform 3 is implicated in the G2/M cell cycle arrest and its overexpression has the opposite effect on

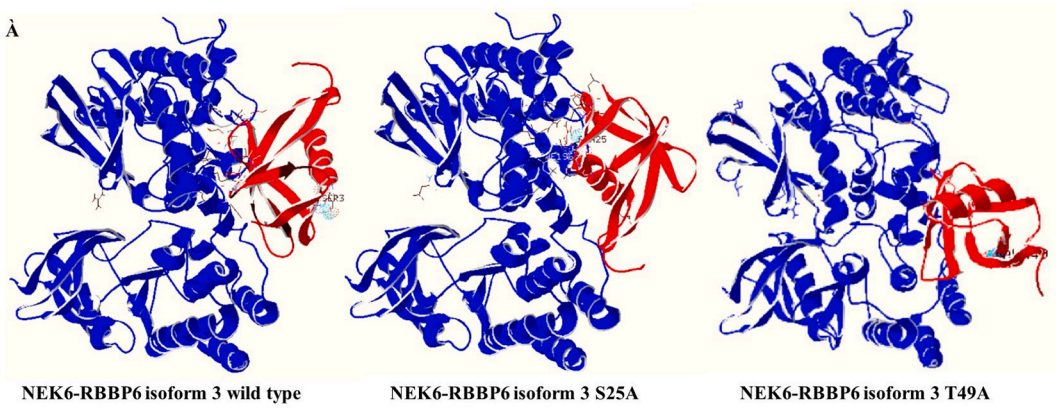

Fig. 6. Docking models for interactions between NEK6 and mutants of RBBP6 isoform 3 and predicted phosphorylation sites in RBBP6 isoform 3. (A) The amino acid substitutions in the mutants of RBBP6 isoform 3 do not alter the 3D structure of the protein. However, these changes result in completely different interactions between NEK6 and the mutants. **(B)** The amino acid sequence of RBBP6 isoform 3, showing the predicted phosphorylation sites.

Table 2
Energy and model numbers for Nek6 and RBBP6 isoform 3 docking models.

	Clusters	Centre	Lowest energy	Clusters	Centre	Lowest energy
RBBP6 -3	91	−636.6	−681.3	99	−622.2	−759.7
S25A	86	−552.9	−635.5	106	−618.7	−699.1
T49A	82	−578.3	−586.2	106	−619.5	−691.8

cell cycle by allowing progression [22,89]. Attributed to its involvement in cell cycle regulation, these results demonstrate that targeting RBBP6 isoform 3 phosphorylation could serve as a potential therapeutic target for cancer.

In this study, we were able to show the interaction between Nek6 and the DWNN domain. NEK 6 is a protein kinase that is involved in chromosome segregation and promotes cell cycle progression. It is known to phosphorylate RBBP6 [66,91]. This interaction may therefore result in the phosphorylation of the DWNN domain in the isoforms of RBBP6 by Nek6. The phosphorylation of RBBPBBP6 isoform 1 promotes cell

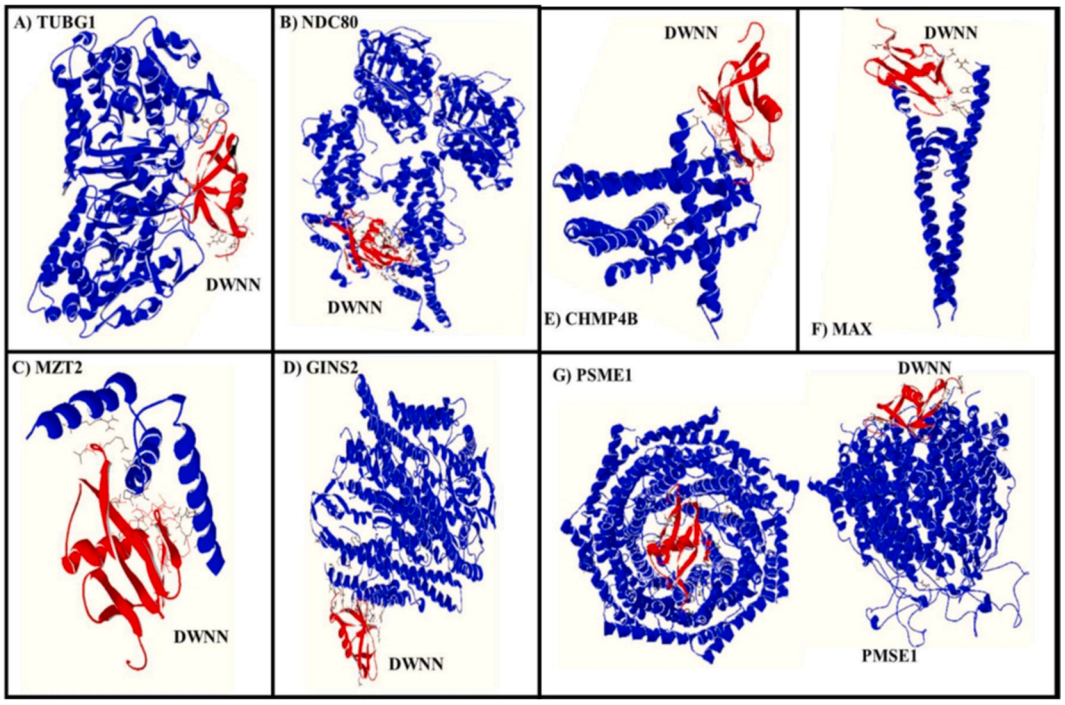

Fig. 7. Cell cycle regulators interacting with RBBP6 isoform 3. These are representations of the ClusPro docking models for the interaction of these cell cycle regulators with RBBP6 isoform 3. (A) TubG1, (B) NDC80, (C) MZT2 and (E) CHPB4 all regulate the cell cycle by interacting with the microtubule during cell division (D) GINS2 and (F) MAX are associated with the DNA replication complex. (G) PSME1 is a negative regulator of cell cycle progression.

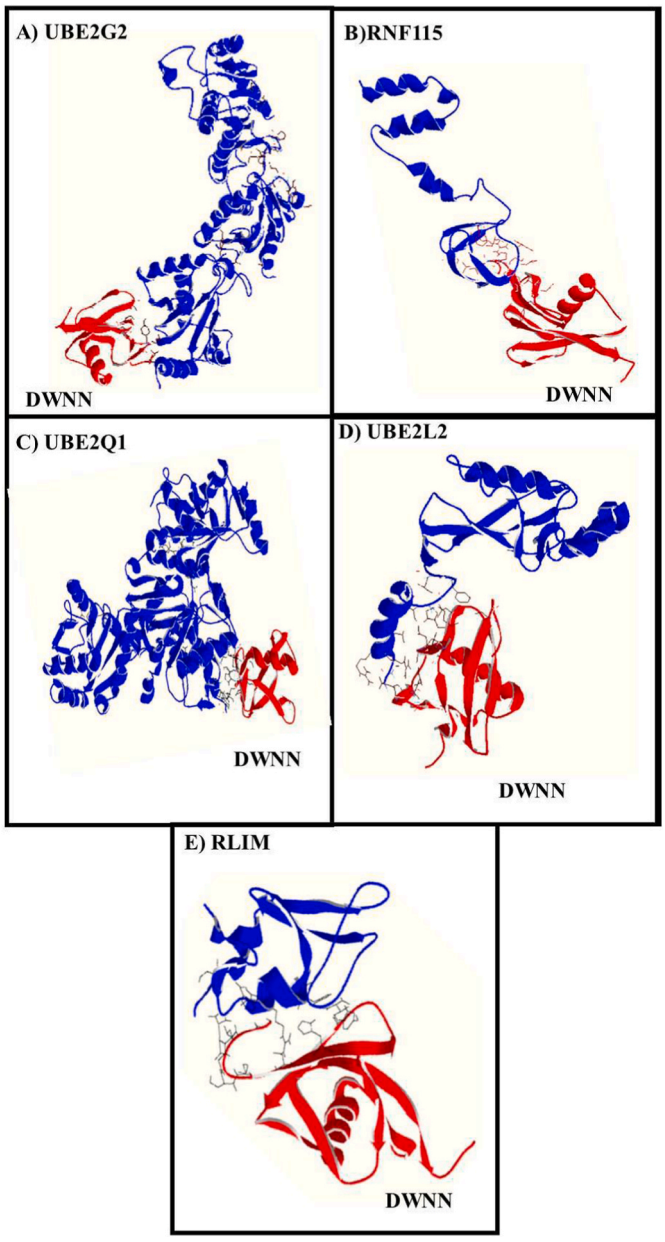

Fig. 8. Ubiquitin ligases interacting with RBBP6 isoform 3. These are representations of the ClusPro models for the interaction of these ubiquitin ligases with RBBP6 isoform 3. Three of them are E2 ligases (A, C and D) while the remaining two are E3 ligases (B and E).

proliferation. Our study identified 17 probable phosphorylation sites in the sequence of RBBP6 isoform 3. The association of RBBP6 with cancer is well documented. Nek6 is also known to play a significant role in cancer progression and is often upregulated in most advanced cancers such as breast, liver, prostate, gastric and colorectal cancer [89]. Nek6 has previously been implicated in the transforming growth factor beta (TGFβ) pathway. Using hepatocellular carcinoma as a model disease, Zuo et al. showed that the overexpression of Nek6 suppresses transcription activity mediated by the TGFβ pathway and the arrest of cell progression [92]. The overexpression of Nek6 is attributed to enhanced cell progression by suppressing the G2/M cell cycle arrest. Targeting the expression of Nek6 could have the opposite effect [93]. Moreover, Jee et al. confirmed that the downregulation of Nek6 is required to activate G2/M cell cycle arrest following DNA damage [94]. Our results indicate that phosphorylation of RBBP6 isoform 1 at its/DWNN domain by Nek6 promotes cell proliferation as reduced affinity was seen in the DWNN mutants. Since the nuclear localization of RBBP6 isoform 3 increases to response to cell stress, we suggest that this isoform serves as a regulatorby associating with Nek6 via its DWNN domain and inhibiting the ability of Nek6 to associate with RBBP6 isoform 1 via its DWNN domain. These results suggest the interaction of RBBP6 isoform 3/DWNN and Nek6 can serve as targets for novel anti-cancer therapy.

We have identified 11 other proteins involved in cell cycle regulation that could potentially be related to DWNN with functions in the cell cycle. By analyzing ClusPro models of these proteins interacting with DWNN, 7 were identified to form bonds with DWNN with bond lengths within 6 Å. Two with the lowest energy of interaction were both proteins that associated with microtubules during cell proliferation. Tubulin, gamma 1 (TUBG1), a member of the tubulin family, binds to microtubules at the centrosome, facilitating microtubule formation. This has been shown to result in cell division and progression of the cell cycle [95]. RBBP6 may prevent the degradation of this protein allowing for the protein to remain active within the cell. NDC80 is a component of the kinetochore and binds to the microtubule. It is involved in spindle checkpoint signalling, detecting if chromosome segregation is proceeding correctly. NDC80 is known to interact with members of the NEK family. This may provide a clue as to the function performed by RBBP6 isoform 3 binding to this protein [96,97]. Two of these proteins GINS2 and MAX are associated with the DNA replication complex. GINS2 promotes DNA replication by promoting the extension of the replication fork. Recently, GINS2 has been identified as a biomarker for cervical cancer and implicated in cancer progression. GINS2 plays a vital role in DNA replication and cell proliferation is observed in patients with low levels of GINS2 and also inhibiting metastases [88,98]. MAX is a transcriptional regulator and binds to other transcription factors and either promoting or inhibiting the transcription of specific genes. One of the target genes that can either be up or down regulated depending on the transcription factor that MAX binds to is the *Myc* oncogene [99]. The role played by RBBP6 isoform 3 associating with MAX would need to be established as this isoform normally acts as a cancer suppressor. The final protein in this group is a proteasome component, Proteosome activator subunit complex1 (PSME1). This protein is a negative regulator of the cell cycle. It and other members of the PSME family are found to be up-regulated in skin cancer [100] and acute lymphoblastic leukaemia [101]. In an unpublished data, RBBP6 isoform 3 is highly expressed in Jurkat cells and this interaction requires further interrogation.

Of the identified cell cycle regulator proteins that do not form bonds within the 6 Å cutoff, the Polo-like kinase 2 (PLK2) protein is mostly expressed in the G2/M phases of the cell cycle. It is actively involved in mitosis, cytokinesis and centriole duplication [102], a function similarly to Nek6 in mitotic progression. Inhibition of Nek6 impedes cell cycle-related activities and could result in mitotic arrest, spindle defects and apoptosis [103,104]. Addition to cell cycle regulation, proteins overexpressed in cancer could serve as potential biomarkers or targets for drug development. One of these proteins, Smad3, has been shown to be downregulated in cancer. Smad3 is involved in TGF-β signaling pathway, well-established in cancer. Daly et al. demonstrated low levels of Smad3 in highly proliferative cancer cells [105]. By activating the up-regulation of Smad3, tumor proliferation could be controlled through the activation of the TGF-β signaling pathway.

The interaction of RBBP6 isoform 3 with both E3 and E2 ligases is unsurprising. If the existence of a protein that is composed almost entirely of the ubiquitin like DWNN domain implies that this is a new type of modification (DWNNylation), then the DWNN domain would bind to both E2 and E3 ligases as part of the DWNNylation chain, similar to the ubiquitination chain. Alternately, the binding of DWNN to these proteins may serve to block Ubiquitin from binding to them. In this way, RBBP6 isoform 3 may be preventing ubiquitination and the resulting protein degradation.

Taken together, the potential interaction of these proteins with RBBP6 isoform 3/DWNN indicates its role in tumor progression through

Table 3
ClusPro docking results for cell cycle regulators and ubiquitin ligases that interact with RBBP6 isoform 3 with identified probable interacting residues.

Protein	Uniprot accession	PDB ID	Balanced scores			Electrostatic scores		
			Clusters	Centre	Lowest energy	Clusters	Centre	Lowest energy
NEK6	Q9HC98		135	−679.6	−719.3	99	−622.2	−759.7
TUBG1	P23258	6V5V	102	−687.2	−812.2	90	−779	−945.2
NDC80	O14777	31Z0	54	−733.4	−810.4	71	−715.4	−904.5
UBE2G2	P60604	2CYX	53	−639.9	−639.9	61	−713.5	−830.4
MZT2	Q6NZ67	None	78	−629.6	−647.4	70	−656.9	−658
GINS2	Q9brt9	None	62	−625.9	−678.4	45	−663.9	−767.7
RNF115	Q9Y4L5	None	166	−630.8	−646.5	140	−591.6	−709.1
CHMP4B	Q9H444	4ABM	138	−585.8	−610.3	152	−672.4	−682.1
MAX	P61244	None	47	−484.6	−594.	45	−587	−679.3
UBE2Q1	Q7Z7E8	2QGX	158	−502.3	−591.5	237	−575.4	−649.7
PMSE1	Q06323	1AVO	46	−476.5	−581.4	40	−546.8	−640.9
UBE2L2	Q7Z7E8	None	58	−503.2	−545.8	58	−520.3	−635.2
RLIM	Q9NVW2	None	114	−455.4	−561.3	95	−527.4	−552.4

the cell cycle regulation rendering these proteins as targets for novel anticancer therapies. Interactions between DWNN and these proteins require further validations. It is important to note that as all the isoforms of RBBP6 have the DWNN domain, all the isoforms can interact with the identified proteins. However, the interaction of isoform 3 with these proteins may serve to regulate the interaction of the other isoforms with these proteins by competing for binding sites. Additionally, if these proteins are a target for DWNNYlation, Isoform3 may not only inhibit the binding of the other RBBP6 isoforms to the identified proteins but may also lead to their degradation.

In conclusion, the interaction of RBBP6 isoform 3/DWNN and Nek6 could promote tumorigenesis through cell proliferation. Therapeutic agents or inhibitors that can induce inhibitory effects of the interaction of RBBP6 isoform 3/DWNN and Nek6 can potentially reverse the effects and serve as novel anti-cancer strategies.

Declaration of competing interest

Authors declare that there is no conflict of interest.

Acknowledgments

We thank the South African Medical Research Council (SAMRC) and the National Research Foundation (NRF) for funding this project.

Appendix A. Supplementary data

Supplementary data to this article can be found online at https://doi.org/10.1016/j.imu.2021.100522.

References

[1] Pugh DJ, et al. DWNN, a novel ubiquitin-like domain, implicates RBBP6 in mRNA processing and ubiquitin-like pathways. BMC Struct Biol 2006;6:1.
[2] Jones C, Reifegerste R, Moses K. Characterization of Drosophila mini-me, a gene required for cell proliferation and survival. Genetics 2006;173(2):793–808.
[3] Di Giammartino DC, et al. RBBP6 isoforms regulate the human polyadenylation machinery and modulate expression of mRNAs with AU-rich 3' UTRs. Genes Dev 2014;28(20):2248–60.
[4] Vo LT, et al. Mpe1, a zinc knuckle protein, is an essential component of yeast cleavage and polyadenylation factor required for the cleavage and polyadenylation of mRNA. Mol Cell Biol 2001;21(24):8346–56.
[5] Li L, et al. PACT is a negative regulator of p53 and essential for cell growth and embryonic development. Proc Natl Acad Sci U S A 2007;104(19):7951–6.
[6] Chibi M, et al. RBBP6 interacts with multifunctional protein YB-1 through its RING finger domain, leading to ubiquitination and proteosomal degradation of YB-1. J Mol Biol 2008;384(4):908–16.
[7] Miotto B, et al. The RBBP6/ZBTB38/MCM10 axis regulates DNA replication and common fragile site stability. Cell Rep 2014;7(2):575–87.
[8] Saijo M, et al. Molecular cloning of a human protein that binds to the retinoblastoma protein and chromosomal mapping. Genomics 1995;27(3):511–9.
[9] Sakai Y, et al. cDNA sequence and chromosomal localization of a novel human protein, RBQ-1 (RBBP6), that binds to the retinoblastoma gene product. Genomics 1995;30(1):98–101.
[10] Simons A, et al. PACT: cloning and characterization of a cellular p53 binding protein that interacts with Rb. Oncogene 1997;14(2):145–55.
[11] Witte MM, Scott RE. The proliferation potential protein-related (P2P-R) gene with domains encoding heterogeneous nuclear ribonucleoprotein association and Rb1 binding shows repressed expression during terminal differentiation. Proc Natl Acad Sci U S A 1997;94(4):1212–7.
[12] Mather A, Rakgotho M, Ntwasa M. SNAMA, a novel protein with a DWNN domain and a RING finger-like motif: a possible role in apoptosis. Biochim Biophys Acta 2005;1727(3):169–76.
[13] Huang P, et al. The C. elegans Homolog of RBBP6 (RBPL-1) regulates fertility through controlling cell proliferation in the germline and nutrient synthesis in the intestine. PloS One 2013;8(3):e58736.
[14] Gao S, Scott RE. P2P-R protein overexpression restricts mitotic progression at prometaphase and promotes mitotic apoptosis. J Cell Physiol 2002;193(2):199–207.
[15] Scott RE, et al. Functional potential of P2P-R: a role in the cell cycle and cell differentiation related to its interactions with proteins that bind to matrix associated regions of DNA? J Cell Biochem 2003;90(1):6–12.
[16] Pretorius A, et al. Silencing of mouse RBBP6 using interference RNA implicates it in apoptosis and the cell cycle. 2013;2(2):50.
[17] Moela P, Motadi LR. RBBP6: a potential biomarker of apoptosis induction in human cervical cancer cell lines. Onco Targets Ther 2016;9:4721–35.
[18] Morisaki T, et al. Comparative proteomics analysis of gastric cancer stem cells. PloS One 2014;9(11):e110736.
[19] Chen J, et al. Overexpression of RBBP6, alone or combined with mutant TP53, is predictive of poor prognosis in colon cancer. PloS One 2013;8(6):e66524.
[20] Motadi LR, Bhoola KD, Dlamini Z. Expression and function of retinoblastoma binding protein 6 (RBBP6) in human lung cancer. Immunobiology 2011;216(10):1065–73.
[21] Yoshitake Y, et al. Proliferation potential-related protein, an ideal esophageal cancer antigen for immunotherapy, identified using complementary DNA microarray analysis. Clin Canc Res 2004;10(19):6437–48.
[22] Dlamini Z, et al. RBBP6 is abundantly expressed in human cervical carcinoma and may Be implicated in its malignant progression. Biomarkers Canc 2019;11.1179299x19829149.
[23] Dlamini Z, et al. Expression analysis and association of RBBP6 with apoptosis in colon cancers. J Mol Histol 2016;47(2):169–82.
[24] Mbita Z, et al. De-regulation of the RBBP6 isoform 3/DWNN in human cancers. Mol Cell Biochem 2012;362(1–2):249–62.
[25] Uhlén M, et al. Proteomics. Tissue-based map of the human proteome. Science 2015;347(6220):1260419.
[26] Szmyd-Potapczuk AV. Investigation of the intra-cellular localisation of Retinoblastoma Binding Protein 6 using immunofluorescence microscopy. 2017.
[27] Fu XD, Maniatis T. Factor required for mammalian spliceosome assembly is localized to discrete regions in the nucleus. Nature 1990;343(6257):437–41.
[28] Sacco-Bubulya P, Spector DL. Disassembly of interchromatin granule clusters alters the coordination of transcription and pre-mRNA splicing. J Cell Biol 2002;156(3):425–36.
[29] Meirelles GV, et al. Human Nek6 is a monomeric mostly globular kinase with an unfolded short N-terminal domain. BMC Struct Biol 2011;11:12.
[30] Chatr-Aryamontri A, et al. The BioGRID interaction database: 2017 update. Nucleic Acids Res 2017;45(D1):D369–d379.
[31] Stark C, et al. BioGRID: a general repository for interaction datasets. Nucleic Acids Res 2006;34(Database issue):D535–9.
[32] Xenarios I, et al. DIP: the database of interacting proteins. Nucleic Acids Res 2000;28(1):289–91.
[33] Prasad TS, Kandasamy K, Pandey A. Human protein reference database and human proteinpedia as discovery tools for systems biology. Methods Mol Biol 2009;577:67–79.

[34] Breuer K, et al. InnateDB: systems biology of innate immunity and beyond–recent updates and continuing curation. Nucleic Acids Res 2013;41(Database issue): D1228–33.
[35] Kerrien S, et al. The IntAct molecular interaction database in 2012 2012;40(D1): D841–6.
[36] Snel B, et al. STRING: a web-server to retrieve and display the repeatedly occurring neighbourhood of a gene. Nucleic Acids Res 2000;28(18):3442–4.
[37] Franceschini A, et al. STRING v9.1: protein-protein interaction networks, with increased coverage and integration. Nucleic Acids Res 2013;41(Database issue): D808–15.
[38] The UniProt Consortium. The universal protein resource (UniProt) 2009. Nucleic Acids Res 2009;37(Database issue):D169–74.
[39] Kanehisa M, Goto S. KEGG: kyoto encyclopedia of genes and genomes. Nucleic Acids Res 2000;28(1):27–30.
[40] Finn RD, et al. The Pfam protein families database: towards a more sustainable future. Nucleic Acids Res 2016;44(D1):D279–85.
[41] Marchler-Bauer A, et al. CDD/SPARCLE: functional classification of proteins via subfamily domain architectures. Nucleic Acids Res 2017;45(D1):D200–d203.
[42] Marchler-Bauer A, Bryant SH. CD-Search: protein domain annotations on the fly. Nucleic Acids Res 2004;32(Web Server issue):W327–31.
[43] Wong YH, et al. KinasePhos 2.0: a web server for identifying protein kinase-specific phosphorylation sites based on sequences and coupling patterns. Nucleic Acids Res 2007;35(Web Server issue):W588–94.
[44] Blom N, et al. Prediction of post-translational glycosylation and phosphorylation of proteins from the amino acid sequence. Proteomics 2004;4(6):1633–49.
[45] Söding J, Biegert A, Lupas AN. The HHpred interactive server for protein homology detection and structure prediction. Nucleic Acids Res 2005;33(Web Server issue):W244–8.
[46] Pei J, Kim BH, Grishin NV. PROMALS3D: a tool for multiple protein sequence and structure alignments. Nucleic Acids Res 2008;36(7):2295–300.
[47] Sali A, Blundell TL. Comparative protein modelling by satisfaction of spatial restraints. J Mol Biol 1993;234(3):779–815.
[48] Fiser A, Do RKG, Šali AJPs. Modeling of loops in protein structures. 2000;9(9): 1753–73.
[49] Ho BK, Brasseur R. The Ramachandran plots of glycine and pre-proline. BMC Struct Biol 2005;5:14.
[50] Lovell SC, et al. Structure validation by Calpha geometry: phi,psi and Cbeta deviation. Proteins 2003;50(3):437–50.
[51] Eisenberg D, Lüthy R, Bowie JU. VERIFY3D: assessment of protein models with three-dimensional profiles. Methods Enzymol 1997;277:396–404.
[52] Sippl MJ. Recognition of errors in three-dimensional structures of proteins. Proteins 1993;17(4):355–62.
[53] Comeau SR, et al. ClusPro: a fully automated algorithm for protein-protein docking. Nucleic Acids Res 2004;32(Web Server issue):W96–9.
[54] Kozakov D, et al. The ClusPro web server for protein-protein docking. Nat Protoc 2017;12(2):255–78.
[55] Dominguez C, Boelens R, Bonvin AM. HADDOCK: a protein-protein docking approach based on biochemical or biophysical information. J Am Chem Soc 2003; 125(7):1731–7.
[56] van Zundert GCP, et al. The HADDOCK2.2 web server: user-friendly integrative modeling of biomolecular complexes. J Mol Biol 2016;428(4):720–5.
[57] Malhotra S, Mathew OK, Sowdhamini R. DOCKSCORE: a webserver for ranking protein-protein docked poses. BMC Bioinf 2015;16(1):127.
[58] de Beer TA, et al. PDBsum additions. Nucleic Acids Res 2014;42(Database issue): D292–6.
[59] Laskowski RA. PDBsum: summaries and analyses of PDB structures. Nucleic Acids Res 2001;29(1):221–2.
[60] Tina KG, Bhadra R, Srinivasan N. PIC: protein interactions calculator. Nucleic Acids Res 2007;35(Web Server issue):W473–6.
[61] Blom N, Gammeltoft S, Brunak S. Sequence and structure-based prediction of eukaryotic protein phosphorylation sites. J Mol Biol 1999;294(5):1351–62.
[62] Lynn DJ, et al. InnateDB: facilitating systems-level analyses of the mammalian innate immune response. Mol Syst Biol 2008;4:218.
[63] Kerrien S, et al. IntAct–open source resource for molecular interaction data. Nucleic Acids Res 2007;35(Database issue):D561–5.
[64] Keshava Prasad TS, et al. Human protein reference database–2009 update. Nucleic Acids Res 2009;37(Database issue):D767–72.
[65] Colland F, et al. Functional proteomics mapping of a human signaling pathway. Genome Res 2004;14(7):1324–32.
[66] Vaz Meirelles G, et al. Characterization of hNek6 interactome reveals an important role for its short N-terminal domain and colocalization with proteins at the centrosome. J Proteome Res 2010;9(12):6298–316.
[67] Wang J, et al. Protein interaction data set highlighted with human Ras-MAPK/PI3K signaling pathways. J Proteome Res 2008;7(9):3879–89.
[68] Ding X, et al. Mixed lineage leukemia 5 (MLL5) protein stability is cooperatively regulated by O-GlcNac transferase (OGT) and ubiquitin specific protease 7 (USP7). PloS One 2015;10(12):e0145023.
[69] Hein MY, et al. A human interactome in three quantitative dimensions organized by stoichiometries and abundances. Cell 2015;163(3):712–23.
[70] Huttlin EL, et al. The BioPlex network: a systematic exploration of the human interactome. Cell 2015;162(2):425–40.
[71] Jung SY, et al. Proteomic analysis of steady-state nuclear hormone receptor coactivator complexes. Mol Endocrinol 2005;19(10):2451–65.
[72] Stehling O, et al. MMS19 assembles iron-sulfur proteins required for DNA metabolism and genomic integrity. Science 2012;337(6091):195–9.
[73] Varjosalo M, et al. The protein interaction landscape of the human CMGC kinase group. Cell Rep 2013;3(4):1306–20.
[74] Elzi DJ, et al. Proteomic analysis of the EWS-fli-1 interactome reveals the role of the lysosome in EWS-fli-1 turnover. J Proteome Res 2014;13(8):3783–91.
[75] Havugimana PC, et al. A census of human soluble protein complexes. Cell 2012; 150(5):1068–81.
[76] Wan C, et al. Panorama of ancient metazoan macromolecular complexes. Nature 2015;525(7569):339–44.
[77] Di Giammartino DC, Manley JL. New links between mRNA polyadenylation and diverse nuclear pathways. Mol Cell 2014;37(9):644–9.
[78] Peidis P, et al. Systems genetics analyses predict a transcription role for P2P-R: molecular confirmation that P2P-R is a transcriptional co-repressor. BMC Syst Biol 2010;4:14.
[79] Gautier VW, et al. In vitro nuclear interactome of the HIV-1 Tat protein. Retrovirology 2009;6:47.
[80] Kappo MA, et al. Solution structure of RING finger-like domain of retinoblastoma-binding protein-6 (RBBP6) suggests it functions as a U-box. 2012;287(10): 7146–58.
[81] Huttlin EL, et al. Architecture of the human interactome defines protein communities and disease networks. Nature 2017;545(7655):505–9.
[82] Deriziotis P. S.J.J.B.e.B.A.-M.B.o.D. Tabrizi. Prions and the proteasome. 2008; 1782(12):713–22.
[83] Kerscher O, Felberbaum R, Hochstrasser M. Modification of proteins by ubiquitin and ubiquitin-like proteins. Annu Rev Cell Dev Biol 2006;22:159–80.
[84] Pfleger CM, et al. Inhibition of Cdh1-APC by the MAD2-related protein MAD2L2: a novel mechanism for regulating Cdh1. Genes Dev 2001;15(14):1759–64.
[85] Yarm FR. Plk phosphorylation regulates the microtubule-stabilizing protein TCTP. Mol Cell Biol 2002;22(17):6209–21.
[86] Richards MW, et al. An autoinhibitory tyrosine motif in the cell-cycle-regulated Nek7 kinase is released through binding of Nek9. Mol Cell 2009;36(4):560–70.
[87] Srinivasan P, Chella Perumal P, Sudha A. Discovery of novel inhibitors for Nek6 protein through homology model assisted structure based virtual screening and molecular docking approaches. ScientificWorldJournal 2014;2014:967873.
[88] Zhang QH, et al. Cloning and functional analysis of cDNAs with open reading frames for 300 previously undefined genes expressed in CD34+ hematopoietic stem/progenitor cells. Genome Res 2000;10(10):1546–60.
[89] Ntwasa M. N.E., cajee UF, the retinoblastoma binding protein 6 family is essential for embryonic development and carcinogenesis. Journal of Cancer Research Forecast 2018;1(1):1002.
[90] Xiao C, et al. RBBP6, a RING finger-domain E3 ubiquitin ligase, induces epithelial-mesenchymal transition and promotes metastasis of colorectal cancer. Cell Death Dis 2019;10(11):833.
[91] Li MZ, et al. Assignment of NEK6, a NIMA-related gene, to human chromosome 9q33. 3–>q34.11 by radiation hybrid mapping. Cytogenet Cell Genet 1999;87 (3–4):271–2.
[92] Zuo J, et al. An inhibitory role of NEK6 in TGFbeta/Smad signaling pathway. BMB Rep 2015;48(8):473–8.
[93] de Oliveira AP, et al. Checking NEKs: overcoming a bottleneck in human diseases. Molecules 2020;25(8):1778.
[94] Jee HJ, et al. Nek6 suppresses the premature senescence of human cancer cells induced by camptothecin and doxorubicin treatment. Biochem Biophys Res Commun 2011;408(4):669–73.
[95] Maounis NF, et al. Expression of γ-tubulin in non-small cell lung cancer and effect on patient survival. Histol Histopathol 2019;34(1):81–90.
[96] Ciferri C, Musacchio A, Petrovic A. The Ndc80 complex: hub of kinetochore activity. FEBS Lett 2007;581(15):2862–9.
[97] Chen Y, et al. Phosphorylation of the mitotic regulator protein Hec1 by Nek2 kinase is essential for faithful chromosome segregation. J Biol Chem 2002;277 (51):49408–16.
[98] Ouyang F, et al. GINS2 is a novel prognostic biomarker and promotes tumor progression in early-stage cervical cancer. Oncol Rep 2017;37(5):2652–62.
[99] Comino-Méndez I, et al. Functional and in silico assessment of MAX variants of unknown significance. J Mol Med (Berl) 2015;93(11):1247–55.
[100] Wang Q, et al. The prognostic value of the proteasome activator subunit gene family in skin cutaneous melanoma. J Canc 2019;10(10):2205–19.
[101] Dehghan-Nayeri N, et al. Differential expression pattern of protein markers for predicting chemosensitivity of dexamethasone-based chemotherapy of B cell acute lymphoblastic leukemia. Canc Chemother Pharmacol 2017;80(1):177–85.
[102] Cizmecioglu O, et al. Plk2 regulates centriole duplication through phosphorylation-mediated degradation of Fbxw7 (human Cdc4). J Cell Sci 2012; 125(Pt 4):981–92.
[103] De Donato M, et al. Identification and antitumor activity of a novel inhibitor of the NIMA-related kinase NEK6. Sci Rep 2018;8(1):16047.
[104] O'Regan L, Fry AM. The Nek6 and Nek7 protein kinases are required for robust mitotic spindle formation and cytokinesis. Mol Cell Biol 2009;29(14):3975–90.
[105] Daly AC, Vizán P, Hill CS. Smad3 protein levels are modulated by Ras activity and during the cell cycle to dictate transforming growth factor-beta responses. J Biol Chem 2010;285(9):6489–97.